

First measurement of $^{25}\text{Al}+\text{p}$ resonant scattering relevant to the astrophysical reaction $^{22}\text{Mg}(\alpha,\text{p})^{25}\text{Al}$

J. Hu^{1,2,*}, *H. Yamaguchi*^{3,4}, *Y.H. Lam*^{1,2}, *A. Heger*^{5,6,7,8}, *D. Kahl*^{9,10}, *A.M. Jacobs*^{8,11}, *Z. Johnston*^{8,11}, *S.W. Xu*¹, *N.T. Zhang*¹, *S.B. Ma*¹, *L.H. Ru*¹, *E.Q. Liu*¹, *T. Liu*¹, *S. Hayakawa*³, *L. Yang*³, *H. Shimizu*³, *C.B. Hamill*¹⁰, *A. St.J. Murphy*¹⁰, *J. Su*¹², *X. Fang*¹³, *K.Y. Chae*¹⁴, *M.S. Kwag*¹⁴, *S.M. Cha*¹⁴, *N.N. Duy*^{14,15}, *N.K. Uyen*¹⁴, *D.H. Kim*¹⁴, *R.G. Pizzone*¹⁶, *M. La Cognata*¹⁶, *S. Cherubini*¹⁶, *S. Romano*^{16,17,18}, *A. Tumino*^{16,19}, *J. Liang*²⁰, *A. Psaltis*²⁰, *M. Sferrazza*²¹, *D. Kim*²², *Y.Y. Li*^{1,2}, and *S. Kubono*^{3,23}

¹Institute of Modern Physics, Chinese Academy of Sciences, Lanzhou 730000, China.

²School of Nuclear Science and Technology, University of Chinese Academy of Sciences, Beijing 100049, China

³Center for Nuclear Study(CNS), University of Tokyo, RIKEN campus, 2-1 Hirosawa, Wako, Saitama 351-0198, Japan

⁴National Astronomical Observatory of Japan, 2-21-1 Osawa, Mitaka, Tokyo 181-8588, Japan

⁵School of Physics and Astronomy, Monash University, Victoria 3800, Australia

⁶OzGrav-Monash – Monash Centre for Astrophysics, School of Physics and Astronomy, Monash University, VIC 3800, Australia

⁷Center of Excellence for Astrophysics in Three Dimensions (ASTRO-3D), Australia

⁸The Joint Institute for Nuclear Astrophysics, Michigan State University, East Lansing, MI 48824, USA

⁹Extreme Light Infrastructure - Nuclear Physics, IFIN-HH, 077125 Bucharest-Măgurele, Romania

¹⁰SUPA, School of Physics & Astronomy, University of Edinburgh, Edinburgh EH9 3FD, United Kingdom

¹¹Department of Physics and Astronomy, Michigan State University, East Lansing, MI 48824, USA

¹²College of Nuclear Science and Technology, Beijing Normal University, Beijing 100875, China

¹³Sino-French Institute of Nuclear Engineering and Technology, Sun Yat-Sen University, Zhuhai 519082, Guangdong, China

¹⁴Department of Physics, Sungkyunkwan University, Suwon 16419, Korea

¹⁵Institute of Research and Development, Duy Tan University, Da Nang 550000, Vietnam

¹⁶Laboratori Nazionali del Sud-INFN, Via S. Sofia 62, Catania 95123, Italy

¹⁷Dipartimento di Fisica e Astronomia “Ettore Majorana” - Università degli Studi di Catania

¹⁸Centro Siciliano di Fisica Nucleare e Struttura della Materia (CSFNSM)

¹⁹Facoltà di Ingegneria e Architettura, Università degli Studi di Enna “Kore”, Enna 94100, Italy

²⁰Department of Physics & Astronomy, McMaster University, Ontario L8S 4M1, Canada

²¹Département de Physique, Université Libre de Bruxelles, Bruxelles B-1050, Belgium

²²Department of Physics, Ewha Womans University, Seoul 03760, Korea

²³RIKEN Nishina Center, 2-1 Hirosawa, Wako, Saitama 351-0198, Japan

Abstract. Type I X-ray bursts (XRBs) are the most frequently observed thermonuclear explosions in nature. The $^{22}\text{Mg}(\alpha,\text{p})^{25}\text{Al}$ reaction plays a critical role in XRB models. However, experimental information is insufficient to deduce a precise $^{22}\text{Mg}(\alpha,\text{p})^{25}\text{Al}$ reaction rate for the respective XRB temperature range. A new measurement of $^{25}\text{Al}+\text{p}$ resonant scattering was performed up to the astrophysically interested energy region of $^{22}\text{Mg}(\alpha,\text{p})^{25}\text{Al}$. Several resonances

*e-mail: hujunbaggio@impcas.ac.cn

were observed in the excitation functions, and their level properties have been determined based on an R-matrix analysis. In particular, proton widths and spin-parities of four natural-parity resonances above the α threshold of ^{26}Si , which can contribute the reaction rate of $^{22}\text{Mg}(\alpha, p)^{25}\text{Al}$, were first experimentally determined.

1 Introduction

Type I X-ray bursts are the most frequently observed thermonuclear explosions in nature [1–3]. These astrophysical phenomena occur in the envelope of accreting neutron star in low-mass X-ray binary systems [4, 5]. The investigation of X-ray bursts is significant to the understanding of the neutron star's properties and the underlying physics [6]. The bursts are driven by the tripe- α reaction, the αp -process [7] and the rp -process [8, 9]. After the breakout from the hot CNO cycle, the nucleosynthesis path is characterized by the αp -process which is the dominant process in sd-shell nuclei. The αp -process is a sequence of α - and proton-induced reactions that rapidly transport nuclear material, along the neutron deficient side of the stable nuclei, from the CNO cycle toward heavier masses region.

The X-ray light curve is the only direct observable of X-ray bursts, which is affected significantly by the αp -process. According to a recent sensitivity study by Cyburt *et al.* [10], the $^{22}\text{Mg}(\alpha, p)^{25}\text{Al}$ reaction is thought to be the most sensitive one within the αp -process according to the calculation of multi-zone burst model (KEPLER code) and has a prominent impact on the burst light curve. However, the reaction rates were calculated using the statistical models due to the missing of important experimental information.

2 Experimental method

A resonant scattering measurement of $^{25}\text{Al}+p$ has been performed to experimentally examine the $^{22}\text{Mg}(\alpha, p)^{25}\text{Al}$ reaction rates. The experiment was carried out using the CNS radioactive ion beam separator (CRIB) [11], installed by the Center for Nuclear Study (CNS), University of Tokyo, in the RIKEN Accelerator Research Facility. A primary beam of $^{24}\text{Mg}^{8+}$ was accelerated up to 8.0 MeV/u by the AVF cyclotron ($K = 70$) with an average intensity of 1 μA . The primary beam bombarded a liquid-nitrogen-cooled D_2 gas target [12] where a secondary beam of ^{25}Al was produced via the $^{24}\text{Mg}(\text{d}, \text{n})^{25}\text{Al}$ reaction in inverse kinematics. The D_2 gas at 200 Torr and 90 K was confined in a small cell with a length of 80 mm. The entrance and exit windows were made of 2.5 μm thick Havar foils. The ^{25}Al beam was separated by the CRIB separator using the in-flight method. The ^{25}Al beam, with an energy of 142 ± 1 MeV and an average intensity of 2.0×10^5 pps, was then delivered to F3 experimental chamber and bombarded a 150- μm -thick $(\text{CH}_2)_n$ target in which the beam was stopped. The setup at F3 experimental chamber is shown in figure 1, which is quite similar to that used in Ref. [13]

A PPAC (Parallel Plate Avalanche Counter) [14] and a MCP (Micron Channel Plate) [15] were used for measuring time and position information of the beam particles. The beam particles were identified in an event-by-event mode using the abscissa of MCP, and the ToF between MCP and the RF signal provided by the cyclotron. After passing through a Wien-Filter, the ^{25}Al beam purity was typically 70%. Figure 2(a) shows the beam particle identification before the secondary target.

The recoiling light particles were measured using three sets of Si telescopes at average angles of $\theta_{lab} = 0^\circ, 20^\circ$ and 23° , respectively. Each telescope consisted of a 65- μm -thick

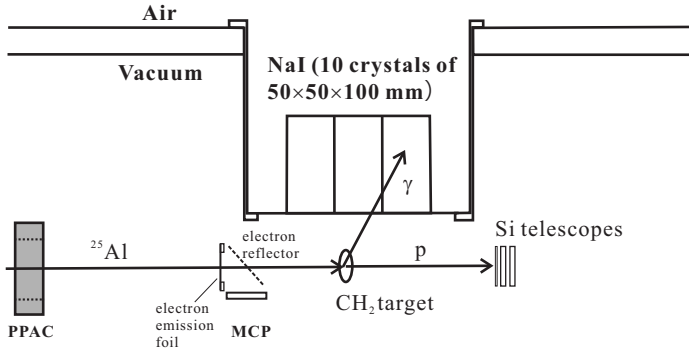


Figure 1. Schematic diagram (side view) of the experimental setup at F3 chamber.

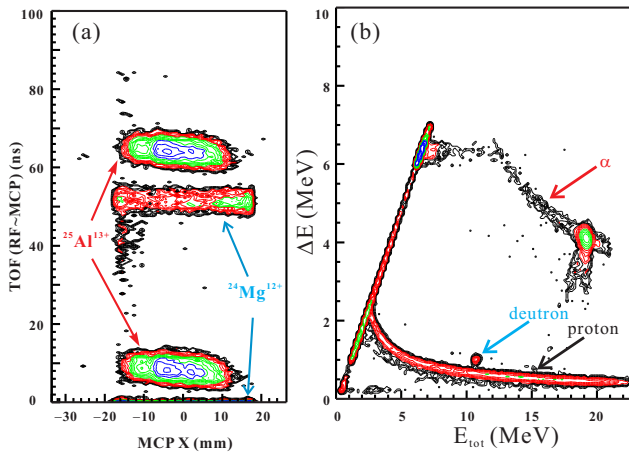


Figure 2. (a) Identification plot for the beams via the ToF technique. (b) Identification plot for the recoiling particles via the ΔE -E technique.

double-side-strip (16×16 strips) silicon detector and two 1500- μm -thick pad detectors. The recoiling particles were clearly identified by using the ΔE -E method as shown in figure 2(b). An array of ten NaI detectors was mounted directly above the target and used to detect the γ rays from the decay of the excited states in ^{25}Al . Each NaI detector is with a geometry of 50 × 50 × 100 mm, covering 20% of the total solid angle altogether. In addition, an 80- μm -thick carbon target was used in a separate run for evaluating the background contribution.

The de-excitation γ rays in the inelastic events have been measured with the NaI detectors. These detectors have an average energy resolution of 13.5% (FWHM) for 662-keV γ rays. The 450-keV photopeak detection efficiency ϵ was measured as 5%, using γ -ray sources placed at the target position. The γ -ray energy spectrum of proton- γ coincident events showed a peak at 450 keV and the contribution to the excitation function by the inelastic scattering events was successfully deduced. The inelastic contribution, less than 12% of the elastic scattering, was subtracted from the total excitation function.

$E_{c.m.}$ resolution of the excitation function was 30-90 keV in full width at half maximum (FWHM) for the Si telescope at $\theta_{lab} = 0^\circ$. The uncertainty was mostly from energy straggling of the particles in the thick target, along with the energy resolution of the silicon detectors. At

larger angles, the angular resolution of the recoiling proton produced large energy uncertainty and the resulting energy resolution was 75-200 keV at $\theta_{lab} \sim 20^\circ$.

3 Experimental results and R-matrix analysis

The excitation function of $^{25}\text{Al}+p$ elastic scattering has been reconstructed using the procedure described previously [13, 16–18]. The excitation function of elastic scattering for the proton target was deduced by subtracting the carbon and inelastic scattering contributions. The excitation function around $\theta_{lab} = 0^\circ$ is shown in figure 3; data from the other two telescopes were not included in the analysis due to their awful energy resolution. Several resonant structures were clearly observed in the spectrum. In order to determine the resonant parameters of observed resonances, R-matrix calculations have been performed with the R-matrix code AZURE2 [19]. A channel radius of $R = 1.4 \times (1 + 25^{1/3}) \approx 5.5$ fm appropriate for the $^{25}\text{Al}+p$ system has been utilized in the calculation.

For the discussions on the level properties obtained by R-matrix analysis and the astrophysical implications on the X-ray bursts, please refer to our published paper [20].

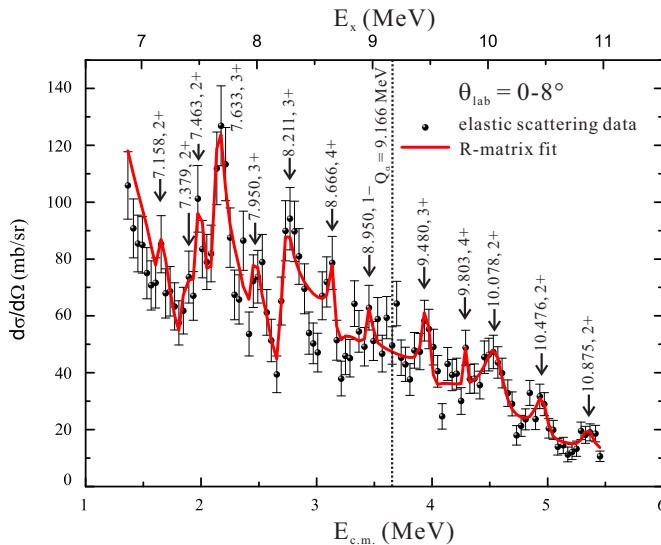


Figure 3. Excitation function of $^{25}\text{Al}+p$ elastic scattering at $\theta_{lab} = 0-8^\circ$. The red curve represents the best overall R-matrix fit.

References

- [1] W.H.G. Lewin et al., *Space Sci. Rev.* **62**, 223 (1993)
- [2] H. Schatz et al., *Nucl. Phys. A* **777**, 601 (2006)
- [3] A. Parikh et al., *Prog. Part. Nucl. Phys.* **69**, 225 (2013)
- [4] S.E. Woosley, R.E. Taam, *Nature* **263**, 101 (1976)
- [5] P.C. Joss, *Nature* **270**, 310 (1977)
- [6] A.W. Steiner et al., *Astrophys. J.* **722**, 33 (2010)
- [7] S.E. Woosley, T.A. Weaver, in *High Energy Transients in Astrophysics, AIP Conf. Proc., vol. 115*, edited by S.E. Woosley (AIP, New York, 1984), p. 273

- [8] R.K. Wallace et al., *Astrophys. J. Suppl.* **45**, 389 (1981)
- [9] M. Wiescher et al., *Astrophys. J.* **316**, 162 (1987)
- [10] R. Cyburt et al., *Astrophys. J.* **830**, 55 (2016)
- [11] Y. Yanagisawa et al., *Nucl. Instr. Meth. A* **539**, 74 (2005)
- [12] H. Yamaguchi et al., *Nucl. Instr. Meth. A* **589**, 150 (2008)
- [13] H. Yamaguchi et al., *Phys. Lett. B* **672**, 230 (2009)
- [14] H. Kumagai et al., *Nucl. Instr. Meth. A* **470**, 562 (2001)
- [15] S. Hayakawa, M. Sc. thesis, Department of Physics, University of Tokyo (2008)
- [16] T. Teranishi et al., *Phys. Lett. B* **556**, 27 (2003)
- [17] T. Teranishi et al., *Phys. Lett. B* **650**, 129 (2007)
- [18] J.J. He et al., *Phys. Rev. C* **76**, 055802 (2007)
- [19] R.E. Azuma et al., *Phys. Rev. C* **81**, 045805 (2010)
- [20] J. Hu et al., *Phys. Rev. Lett.* **127**, 172701 (2021)